Atmospheric Carbonyl Compounds are crucial in Regional Ozone heavy Pollution: Insights from the Chengdu Plain Urban Agglomeration, China

Jiemeng Bao[1,2], Xin Zhang[1,2], Zhenhai Wu[1], Li Zhou[3], Jun Qian[4], Qinwen Tan[5], Fumo Yang[3], Junhui Chen[6], Yunfeng Li[7], Hefan Liu[5], Liqun Deng[6], Hong Li[1*]

[1]Chinese Research Academy of Environmental Sciences, State Key Laboratory of Environmental Benchmarks and Risk Assessment, Beijing 100012, China

[2]School of Environmental Science and Engineering of Peking University, State Key Joint Laboratory of Environmental Simulation and Pollution Control, Joint Laboratory of Regional Pollution Control International Cooperation of the Ministry of Education, Beijing 100871, China

[3]College of Carbon Neutrality Future Technology, Sichuan University, Chengdu 610065, China

[4]Sichuan Radiation Environment Management and Monitoring Central Station, Chengdu 611139, China

[5]Chengdu Academy of Environmental Sciences, Chengdu 610046, China

[6]Sichuan Academy of Eco-Environmental Sciences, Chengdu 610042, China

[7]School of Mechanical Engineering, Beijing Institute of Petrochemical Technology, Beijing 102617,China

Correspondence to: Hong Li (lihong@craes.org.cn)

Abstract. Gaseous carbonyl compounds serve as crucial precursors and intermediates in atmospheric photochemical reactions, significantly contributing to ambient ozone formation. To determine whether the impact of carbonyl compounds on regional ozone pollution is driven by their abundance or by specific secondary chemical processes, simultaneous field observations and observation-based modelling of ambient carbonyls were conducted at nine sites within the Chengdu Plain Urban Agglomeration (CPUA), China during August 4-18, 2019, when three episodes of regional heavy ozone pollution occurred across eight cities within CPUA. Throughout the study, the total mixing ratios of 15 carbonyls ranged from 10.7±4.2 to 35.2±13.4 ppbv. The spatial distribution reveal that regions with higher concentrations of carbonyl compounds, such as around Chengdu, are also areas with more severe ozone pollution. Both the abundance and the chemical reactivity of carbonyl compounds, especially formaldehyde and acetaldehyde,

30 play crucial roles in ozone formation in the CPUA. On ozone pollution days, carbonyl

31 concentrations significantly increased by 22.8% to 66.2%.While the abundance of

32 carbonyls is an important factor, their significant role in heavy ozone pollution within

33 the CPUA is primarily driven by secondary chemical processes, particularly those

34 involving alkenes and BVOCs. Sites with higher average ozone concentrations during

35 observations were mainly in the VOCs-limited regime, while others were in the

36 transitional regime. Additionally, the mutual transport of carbonyl compounds between

37 cities in the CPUA suggests that regional collaboration is essential to address ozone

38 pollution effectively. These findings offer valuable insights for developing effective

39 strategies to control regional ozone pollution.

40 **Keywords:** Gaseous Carbonyls; Ozone Heavy Pollution; Pollution Characteristics;
41 Atmospheric Photochemical Reactivity; Source Analysis; The Chengdu Plain Urban
42 Agglomeration, China

43 **1. Introduction**

44 Atmospheric carbonyl compounds play a pivotal role in tropospheric chemistry,

45 acting as crucial precursors to both ozone (O_3) and secondary organic aerosols (SOA),

46 a fact recognized for decades (Altshuller, 1993; Grosjean and Seinfeld, 1989). Their

47 importance has been confirmed by numerous studies over the years(Guo et al., 2004;

48 Hallquist et al., 2009; Wang et al., 2020; Ye et al., 2021; Coggon et al., 2019),

49 highlighting their significant contribution to atmospheric photochemistry and air

50 pollution. Over the past two decades, severe air pollution in China has driven substantial

51 research efforts to understand the contributions of carbonyl compounds to these

52 environmental challenges. Studies have shown that photolysis of carbonyl compounds

53 is a major source of RO_X radicals (Grosjean and Seinfeld, 1989; Zhang et al., 2016).

54 These compounds can be photolyzed and react with OH radicals to form a large number

55 of HO_2 and RO_2 radicals, which increase the atmospheric oxidation capacity and

56 participate in the NOx photochemical cycle, leading to ozone formation (Zhang et al.,

57 2016; Meng et al., 2017). Additionally, dialdehydes such as glyoxal and methylglyoxal

58   undergo heterogeneous reactions with aqueous particulate matter, rapidly forming SOA

59   (Lou et al., 2010; Xue et al., 2016; Yuan et al., 2012). Ambient carbonyl compounds

60   not only affect the environment but also pose direct health risks to humans. They can

61   harm ecosystems through deposition and adsorption processes (Yang et al., 2018). They

62   also pose direct health risks to humans, including sensitization, carcinogenesis, and

63   mutagenicity (Fuchs et al., 2017).

64   Recent research has increasingly focused on understanding the spatial and

65   temporal variability of carbonyl compounds in highly polluted regions, particularly in

66   China, where rapid industrialization has led to severe air quality challenges. Xue et al.

67   (2013) and Duan et al. (2012) reported typical ambient concentrations of carbonyl

68   compounds ranging from a few $\mu g \cdot m^{-3}$ to tens of $\mu g \cdot m^{-3}$ in urban areas, depending on

69   the specific compounds and regions studied. For example, formaldehyde concentrations

70   in highly polluted areas can exceed 10 $\mu g \cdot m^{-3}$. Shen et al. (2013) and Fu et al. (2008)

71   observed significant diurnal variation, with higher concentrations of carbonyl

72   compounds during the daytime, particularly in the afternoon, driven by photochemical

73   production. Concentrations can increase by as much as 50-100% during peak sunlight

74   hours compared to nighttime levels. Pang and Mu (2006) and Rao et al. (2016)

75   identified key sources of carbonyl compounds, including vehicular emissions, industrial

76   activities, and secondary formation from VOC oxidation in the atmosphere. In urban

77   environments, vehicular emissions are often a dominant primary source, while

78   secondary formation contributes significantly during daytime due to photochemical

79   processes. The results highlight severe and spatiotemporal variations of carbonyl

80   pollution in China. High levels are found mainly in the North China Plain(NCP), the

81   Yangtze River Delta(YRD), and the Pearl River Delta(PRD)(Duan et al., 2008; Shao et

82   al., 2009; Tan et al., 2018; Wang et al., 2018; Xue et al., 2014, 2013; Yang et al., 2017).

83   Urban areas generally exhibit higher carbonyl levels than suburban and rural areas due

84   to human activities(Xue et al., 2013). Despite the progress made, significant gaps

85   remain in understanding the spatiotemporal distribution and source apportionment of

carbonyl compounds, particularly in urban agglomerations. Existing research has primarily focused on urban areas in rapidly developing regions like the NCP, YRD, and PRD. Moreover, studies have often emphasized the overall role of VOCs in ozone pollution, with less attention given to specific carbonyl compounds and their individual contributions to atmospheric oxidation capacity and ozone formation (Meng et al., 2017).

Monitoring carbonyl compounds in the atmosphere is challenging due to their typically low concentrations (ppt-ppb levels), necessitating highly sensitive analytical methods. The diversity of carbonyl compounds, including multiple isomers, requires highly selective analytical techniques for differentiation. Current measurement technologies limit our understanding of the spatiotemporal distribution of carbonyl compounds, affecting the accurate assessment of their environmental behavior, sources, and transport (Xue et al., 2013; Sahu and Saxena, 2015). While numerous studies have explored the role of carbonyl compounds in ozone production, many focus on general mechanisms rather than specific compounds or regional variations (Atkinson and Arey, 2003; Monks et al., 2015).

Atmospheric carbonyl compounds originate from both primary and secondary sources (Pang and Mu, 2006; Rao et al., 2016). Primary sources include the incomplete combustion of fossil fuels and biomass, industrial emissions, emissions from the catering industry, and releases from plants. Secondary sources arise from the atmospheric photochemical oxidation of VOCs (Xue et al., 2013), particularly alkenes, aromatics, and isoprene, which typically dominate the secondary formation of carbonyls. However, distinguishing between primary and secondary contributions remains challenging. Existing source apportionment methods, such as characteristic species ratios and multiple linear regression, often lack the resolution to differentiate these sources accurately, especially for non-vehicular emissions and secondary formation. The limitations of these methods underscore the need for more advanced approaches to better quantify the secondary formation mechanisms of carbonyl

114   compounds and their regional impact on ozone formation. Despite significant

115   advancements in studying atmospheric carbonyls, key gaps remain in understanding

116   their precise spatiotemporal distribution and source apportionment. Specifically, there

117   is a need for studies that examine how carbonyls vary across different environments—

118   urban, suburban, and rural—and during varying pollution events. Without such targeted

119   analysis, our understanding of the behavior of carbonyl compounds and their

120   contribution to ozone pollution remains incomplete, particularly in regions

121   experiencing severe pollution.

122   This study focuses on atmospheric carbonyl compounds and their roles in

123   photochemical pollution within the Chengdu Plain Urban Agglomeration (CPUA) of

124   China. The CPUA includes eight cities: Chengdu, Mianyang, Deyang, Leshan, Meishan,

125   Yaan, Suining, and Ziyang. This region has a developed economy and a high degree of

126   internationalization. The CPUA is located on the western edge of the Sichuan Basin,

127   surrounded by mountain ranges, which easily block airflow. The unique climatic

128   environment of the CPUA features low wind speeds year-round, high frequency of

129   static winds, short hours of sunshine, frequent winter inversions, and a pronounced heat

130   island effect in summer. These climatic characteristics significantly impact the

131   variations in air pollutant concentrations, making the region prone to ozone pollution

132   in summer and haze pollution in winter. (Li et al., 2013; Hu et al., 2017; Zhang et al.,

133   2010). Although previous studies have shown that ozone formation in urban Chengdu

134   is primarily VOCs-limited (Tan et al., 2018), with aromatic hydrocarbons and alkenes

135   contributing significantly to ozone generation in summer (Xu et al., 2020), these studies

136   mainly focus on single cities and overall VOCs. There is still limited understanding of

137   whether the significant roles of carbonyl compounds in ozone formation are primarily

138   due to their abundance or whether specific chemical reactions involving carbonyls drive

139   this process. This study aims to address these gaps by investigating the spatial

140   distribution, sources, and specific chemical pathways of carbonyl compounds across

141   the entire CPUA and assessing their contributions to regional ozone pollution and inter-

142 city air transport mechanisms.

143 To address these research gaps, this study involves an intensive field observation

144 experiment conducted by the Sichuan Academy of Environmental Sciences, Peking

145 University, Sichuan University and Chinese Academy of Environmental Sciences.

146 Atmospheric carbonyl compounds were observed at nine sites in eight cities within the

147 CPUA for 15 days during a period of heavy ozone pollution in August 2019. Samples

148 were analyzed using 2,4-dinitrophenylhydrazine solid phase adsorption/high

149 performance liquid chromatography (HPLC). The study aims to characterize the

150 atmospheric carbonyl compounds in the CPUA, assess their influence on

151 photochemical pollution, identify key carbonyl compounds that may play crucial roles

152 in heavy ozone pollution in the CPUA, and evaluate the contribution of primary

153 emissions, air pollution transport, and secondary generation to key carbonyl compounds

154 through a combination of multivariate linear regression modeling and Observation-

155 Based Modeling (OBM). This research aims to provide technical support for controlling

156 carbonyl compounds pollution in the CPUA and to reduce their contributions to ozone

157 pollution.

158 **2. Materials and methods**

159 **2.1 Observation Sites Profile**

160 In this study, a total of 9 off-line sampling sites for atmospheric carbonyl

161 compounds were set up in 8 cities in the CPUA from August 4th to 18th, 2019(table S1).

162 Considering that this study focused on the pollution characterization of carbonyl

163 compounds in urban areas, one urban site was selected in each city. In addition, in order

164 to compare and study the pollution characteristics of carbonyl compounds in the

165 suburbs, a suburban site was set up in Xinjin County, Chengdu. For the selection of

166 urban sites in each city, priority is given to those choices of set-up in the vicinity of the

167 state-controlled site, and the perimeter of the sites should be open, unobstructed and no

168 obvious pollution sources, with convenient transportation and power supply. The

169   distribution of specific sites is shown in Fig. 1.

170   Ozone concentrations were measured using the UV absorption method with a

171   Thermo O_3 analyzer (Model 49i), with data sourced from national control stations near

172   each sampling site. Nitrogen dioxide (NO_2) was measured by chemiluminescence

173   following chemical conversion to nitric oxide (NO) using a molybdenum catalyst;

174   however, this method is known to have interferences from other NO_z species. Carbon

175   monoxide (CO) was measured via infrared absorption with a Thermo instrument

176   (Model 20). All Thermo instruments were carefully maintained and calibrated daily at

177   01:00 to ensure measurement accuracy. Measurements for ozone, NO_2, and CO were

178   collected with a time resolution of one hour. Simultaneously, meteorological

179   parameters—temperature, relative humidity (RH), wind speed, and direction—were

180   recorded at each observation site using an automatic weather station (PC-4, JZYG,

181   China), also at a one-hour resolution.
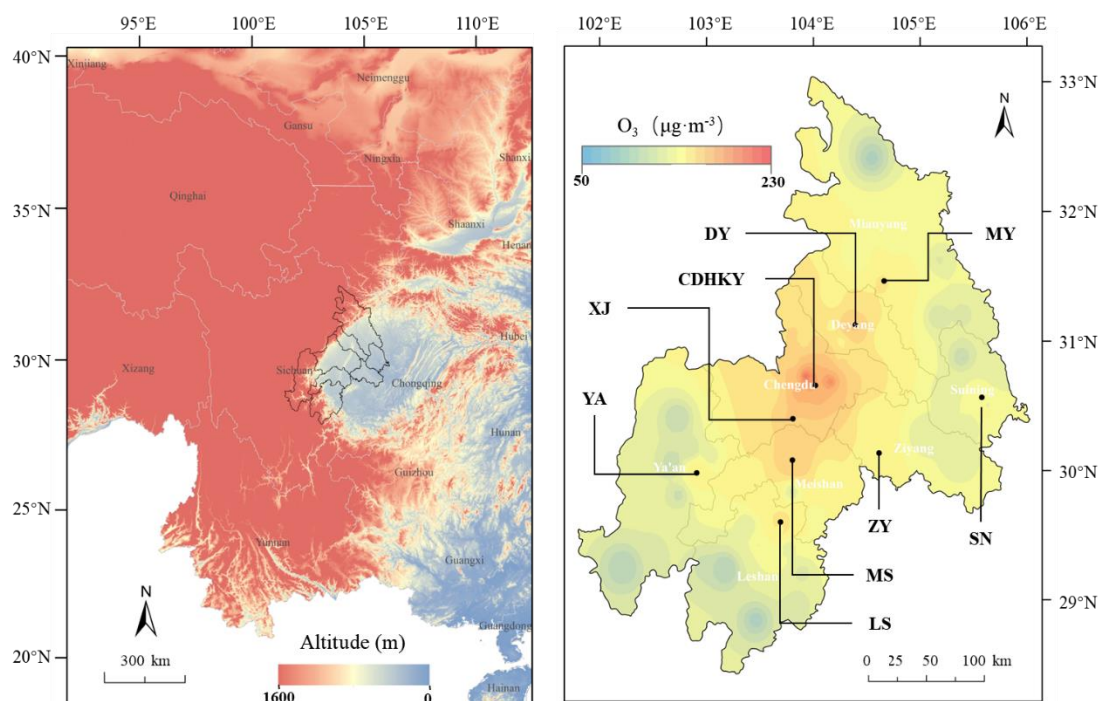
182

183   **Figure 1.** Distribution of sampling sites. The left panel shows the elevation map of the Sichuan

184   Basin, highlighting the geographical features of the region, with elevation data sourced from the

185   Geospatial Data Cloud (https://www.gscloud.cn/#page1/2). The right panel presents the spatial

186   distribution of ozone concentrations in the CPUA during the observation period (August 4–18,

187   2019), with ozone data obtained from national control stations near each sampling site. Black dots

188   represent the locations of the sampling sites, labeled as follows: MY (Mianyang), DY (Deyang),

189 CDHKY (Chengdu Environmental Science Research Institute), XJ (Xinjin), SN (Suining), ZY
190   (Ziyang), MS (Meishan), YA (Ya'an), and LS (Leshan). The color bar in the top left corner
191 corresponds to interpolated ozone concentrations, with each color representing a concentration
192   gradient.

193 **2.2 Samples Collection**

194   The sampling of atmospheric carbonyl compounds mainly referred to the TO-11A

195 standard of the United States Environmental Protection Agency (US EPA) and the

196 Chinese environmental protection standard HJ 683-2014 High Performance Liquid

197 Chromatography Method for the Determination of Atmospheric Carbonyl Compounds,

198 and the sampling was carried out by using silica gel sampling tubes (IC-DN3501 from

199 Tianjin Bonna-Agela) coated with DNPH (2,4-dinitrophenylhydrazine). In this study,

200 an automatic sampler for carbonyl compounds (Zhang et al., 2019) was used to

201 continuously collect atmospheric carbonyl compounds. From August 4th to 18th, 2019,

202 air samples were collected every 2 hours with a sampling flow rate of $0.8 \ L \cdot min^{-1}$. In

203 addition, in order to prevent the impact of ozone and rainwater in the atmospheric air

204 on sample collection, a potassium iodide ozone removal column (KI 140 from Tianjin

205 Bonna-Agela) was installed and a water removal agent made by ourselves (Bao et al.,

206 2022; Wang et al., 2020) was added at the front end of the sample tube. Two blank

207 samples were collected before and after the sampling, and blank samples were also

208 collected for different batches of sampling tubes. The samples were frozen at -18°C and

209 analyzed within one month.

210   Atmospheric VOCs were sampled using SUMMA tanks, stainless steel tanks with

211 electropolished and silanized inner walls, manufactured by Entech in the United States,

212 with a sampling volume of 3.2 liters. The sampling was controlled by a constant current

213 integral sampler to sampling for an average of 1 hour. From August 4th to 18th, 2019,

214 two VOCs samples were collected each day at each site, at 8:00-9:00 and 14:00-15:00

215 (no samples were taken under special weather conditions, such as rain). On August 11th,

216 12th and 16th , six samples were collected per day to capture diurnal variations under

217 ozone pollution events, at the following times: 8:00-9:00, 10:00-11:00, 12:00-13:00,

218 14:00-15:00, 16:00-17:00, and 18:00-19:00.

219 **2.3 Samples Analysis**

220 The carbonyl compounds samples were qualitatively and quantitatively analyzed

221 by using High Performance Liquid Chromatography (HPLC) (LC-20AD, Shimadzu,

222 Japan) and an ultraviolet detector (SPD-20A, Shimadzu, Japan), mainly based on the

223 US EPA TO-11A standard and the Chinese HJ 683-2014 standard. The DNPH sampling

224 column after sampling was slowly eluted into a volumetric flask using acetonitrile

225 (chromatographically pure, Thermo Fisher Scientific China) to 5.0 mL. Then 1.5 mL of

226 the sample was transferred into an HPLC sample bottle, and sealed and stored in a

227 refrigerator at <4 ℃ to complete the pre-treatment. Prior to sample analysis, a standard

228 solution of the concentration gradient was prepared using TO-11A standard solution

229 (Supelco, USA) and used as the external standard. The correlation coefficient (R^2) of

230 the standard curve was greater than 0.995. The detection limit of the device was

231 0.56~5.57 ng·mL^{-1}, and the quantification limit was 1.87~18.56 ng·mL^{-1} (Table S2).

232 Then 20 μL of the pretreated sample was extracted through the autosampler and injected

233 into the HPLC/UV system, detected by a UV detector with a wavelength of 360 nm,

234 qualified by retention time value, quantified by peak area value, and the qualitative and

235 quantitative analysis data of carbonyl compounds were obtained after conversion. The

236 HPLC conditions referred to Chinese environmental protection standard HJ 683-2014:

237 binary gradient washing was performed using acetonitrile and water, 60% acetonitrile

238 was held for 20 mins, acetonitrile was increased linearly from 60% to 100% within 20-

239 30 mins, and acetonitrile was reduced to 60% again within 30-32 mins and held for 8

240 mins; the column oven was kept at 40 ℃. It should be noted that while the sampling

241 and analysis method was effective for most carbonyl compounds, ketones, including

242 methyl vinyl ketone (MVK), were not well sampled during the field observations. As a

243 result, data for MVK and other ketones were missing. During the observation period,

244 DNPH cartridges and HPLC analysis technique were used to detect a total of 15

245   carbonyl compounds (Table S2).

246   The atmospheric VOCs were analyzed using the TO-14 and TO-15 methods,

247   which are recommended by the US EPA. These methods involve frozen

248   preconcentration coupled with gas chromatography and mass spectrometry (GC-MS).

249   TO-15 is a method for detecting and quantifying a wide range of VOCs from air samples.

250   The VOCs were pre-concentrated by the Entech7100 system at a low temperature, then

251   quantified by an Agilent GC-MS. During the sample analysis, four internal standard

252   gases (bromochloromethane, 1,4-difluorobenzene, chlorobenzene-d5, and 4-

253   bromofluorobenzene) were used. A multi-point calibration curve was created using a

254   standard gas containing 118 VOCs, including PAMS compounds, TO-15 target analytes,

255   and carbonyl compounds. PAMS (Photochemical Assessment Monitoring Stations)

256   compounds are a subset of hydrocarbons known to contribute to ozone formation, such

257   as ethane, ethylene, propane, and others.

258   **2.4 Data Analysis**

259   **2.4.1 Ozone pollution assessment criteria**

260   According to the Technical Regulation on Ambient Air Quality Index (on trial),

261   National Environmental Protection Standard of the People's Republic of China HJ

262   633—2012, days with an ozone pollution index (IAQI) of 100 or higher during the

263   observation period were designated as pollution days, while days with an IAQI below

264   100 were considered clean days. This study compared the pollution characteristics of

265   carbonyl compounds between pollution days and clean days. Additionally, the

266   concentrations of formaldehyde, acetaldehyde, and acetone observed during the

267   summer of 2009-2013 in economically developed and industrialized areas such as

268   Beijing, Shanghai, and Guangzhou in China, as well as locations in South America

269   (Brazil), Asia (Thailand), Europe (France), and North America (United States), were

270   selected and compared.

271   **2.4.2 Ozone formation sensitivity**

272   Previous studies have shown that the formaldehyde to NO_2 ratio (FNR) can be

273   used to determine the sensitivity of O_3-NOx-VOCs (Schroeder et al., 2017; Tonnesen

274   and Dennis, 2000; Vermeuel et al., 2019). Most studies used satellite remote sensing-

275   based FNR, but the FNR column concentration ratios inverted by satellite remote

276   sensing mainly represented the average photochemical of the troposphere, and the

277   concentration distributions of HCHO and NO_2 in the vertical direction were

278   inconsistent (Hong et al., 2022; Schroeder et al., 2017). So, there is a large uncertainty

279   to develop ground-level ozone pollution prevention and control measures. In this study,

280   sensitivity analysis of ground-level ozone formation was carried out based on the ratio

281   of ground-level HCHO to NO_2 during the observation period at the 9 sites of 8 cities in

282   the CPUA. FNR < 0.55±0.16 and FNR > 1.0±0.3 were defined to VOCs-limited and

283   NOx-limited, respectively, and FNR ratio ranged from 0.55±0.16 to 1.0±0.3 defined to

284   NO_X and VOCs co-limited (Liu et al., 2021; Zhang et al., 2022).

285   **2.4.3 Exploration of Secondary Formation Mechanisms**

286   **(1) Atmospheric chemical reactivity**

287   In this study, the contribution of atmospheric chemical reactivity of carbonyl

288   compounds to ozone formation was evaluated using the OH free radical consumption

289   rate (L_{OH}) and ozone formation potential (OFP):

290    $$L_{OH} = [OVOC]_i \times k_i(OH) \qquad (1)$$

291   Where, $[OVOC]_i$ was the observed concentration of the ith (i=1 to n) carbonyl

292   compound, in molecule·cm^{-3}; $k_i(OH)$ was the rate constants of the ith carbonyl

293   compound reacting with OH radicals, in cm^3·(molecule·s)$^{-1}$. The unit of L_{OH} is s^{-1},

294   representing the rate of OH radical consumption. The selected $k_i(OH)$ values were from

295   literature (Atkinson and Arey, 2003).

296    $$OFP = MIR_i \times [OVOC]_i \qquad (2)$$

297   Where, MIR was the maximum incremental reactivity of the ith carbonyl

298   compound,in g O_3·(g VOC)$^{-1}$ (grams of ozone formed per gram of volatile organic

299   compound), and the MIR values of each species were from California Code of

300   Regulations (https://govt.westlaw.com); $[OVOC]_i$ was the mass concentration of the ith

301   carbonyl compound, in $\mu g \cdot m^{-3}$. The unit of OFP is $\mu g \cdot m^{-3}$, representing the potential

302   ozone formation.

303   **(2) Observation-based model (OBM)**

304   The Observation-Based Model (OBM) is a box model that uses actual

305   observational data to evaluate the sensitivity of secondary pollutant formation

306   mechanisms to their precursor emissions. By constraining the model with atmospheric

307   observation data, typical secondary pollutants and parameters such as NO_X, SO_2, CO,

308   VOCs, temperature, humidity, pressure, and JNO_2 are input into the model as hourly

309   observational data to calculate the chemical formation and consumption of secondary

310   pollutants and free radicals. In this study, the OBM model used the Master Chemical

311   Mechanism (MCM) (v3.3.1, mcm.leeds.ac.uk), which is a nearly detailed chemical

312   mechanism that describes the chemical processes of 143 VOC species from emission

313   to degradation in the atmosphere, including approximately 6,700 species and 17,000

314   inorganic and organic reactions. In this version of the MCM, a total of 19 carbonyl

315   compounds are included, comprising 9 aldehydes and 10 ketones. Of these, 9 carbonyl

316   compounds were measured in this study, including formaldehyde, acetaldehyde,

317   acetone, propionaldehyde, crotonaldehyde, butyraldehyde, isovaleraldehyde,

318   valeraldehyde, and hexaldehyde. The MCM chemical mechanism can simulate

319   atmospheric photochemical reaction processes under near-real conditions and calculate

320   the concentrations of highly reactive species, quantifying the reaction rates of all

321   species involved. For VOCs, especially carbonyls, that were not directly measured, the

322   MCM uses estimated values derived from emission inventories, literature data, and

323   assumptions based on similar species to provide estimates for their concentrations and

324   reaction rates.

325   Relative Incremental Reactivity (RIR) was first used by Cardelino and Chameides

326   (1995) to simulate the response of ozone to precursor changes through scenario tests

327   using box model calculations. RIR was calculated by assuming that the concentration

328   of a given carbonyl compound precursor decreased by a certain proportion could cause

329   the change of the concentration of the carbonyl compound, so as to further judge the

330   effect of VOCs on the formation of carbonyl compounds. Combining the concentrations

331   and activity levels of 15 carbonyl compounds during the observation period, this study

332   focused on formaldehyde, acetaldehyde, and acetone as the primary research targets.

333   The impacts of various AVOCs(anthropogenic VOCs),including alkanes, alkenes,

334   alkynes, and aromatic hydrocarbons, as well as BVOCs(biogenic VOCs)like isoprene,

335   on the formation of formaldehyde, acetaldehyde, and acetone were assessed using

336   observation-based OBM classification. Specific species of anthropogenic source VOCs

337   (alkanes, alkenes, alkynes, and aromatic hydrocarbons) and biogenic VOCs (isoprene)

338   are detailed in Table S3.

339   VOCs observations, conventional gases (NO_2, CO and SO_2) and meteorological

340   parameters (temperature, relative humidity and pressure) were imputed into the model.

341   It was assumed that the pollutants are well mixed. Under the constraints of the measured

342   hourly concentration data of pollutants, the atmospheric chemical process was

343   simulated to obtain the source-effect relationship of the measured pollutants. By

344   assuming the reduction of the source effect, the RIRs of different carbonyl compounds

345   precursors were calculated, and the sensitivities of carbonyl compounds to different

346   pollutants were obtained, and then the secondary formation mechanism of carbonyl

347   compounds was determined. The formula to calculate the RIR is as follows:

348    $$RIR(X) = \left[\frac{\Delta P_Y(X)/P_Y(X)}{\Delta S(X)/S(X)} \right] \tag{3}$$

349    $$P_Y = Y_{\text{net formation}} - Y_{\text{net consumption}} \tag{4}$$

350   Where X was a specific species; $P_Y(X)$ was the net formation rate of species y;

351   S(X) was the total amount of emissions of species X in a certain period, i.e., the source

352   effect of species X. $\Delta S(X)$ was the change in total emissions of X caused by the

353   hypothetical change in source effect, $\Delta P_Y(X)$ was the change in $P_Y(X)$ after the change

354 in source effect S(X), and RIR(X) was the relative incremental reactivity of species X.

355 The species Y in this study were formaldehyde, acetaldehyde and acetone, respectively,

356 and pollutant X was reduced by 20%.

357   The absolute RIR of the precursor reflects the sensitivity of carbonyl compounds

358 formation to the precursor. The higher the absolute RIR, the more sensitive the carbonyl

359 compounds formation to the precursor. A positive RIR value indicates that reducing the

360 species can reduce the formation rate of species Y, and a negative RIR value indicates

361 that reducing the species can increase the formation rate of species Y.

362 **2.4.4 Sources Analysis**

363 **(1) Multi-linear regression model**

364   There is a good correlation between concentrations of compounds of the same or

365 similar source in the atmosphere. Based on this property, it was assumed that the

366 primary and secondary sources of carbonyl compounds were linearly correlated with

367 the selected tracers, and then a quantitative source model was established by multiple

368 linear statistical regression analysis (Kanjanasiranont et al., 2016a; Li et al., 2010; Ling

369 et al., 2017; Luecken et al., 2012; Lui et al., 2017; Wang et al., 2017). In general, CO is

370 the marker product of typical anthropogenic combustion source emissions, mainly from

371 vehicle exhaust emissions and coal combustion. Ozone, as an indicator of

372 photochemical smog, is a typical secondary formation pollutant. In this study, CO and

373 ozone were selected as the tracers of primary source and secondary source of carbonyl

374 compounds, respectively. The formula is as follows:

375 $$[carbonyl] = \beta_0 + \beta_1[CO] + \beta_2[O_3] \tag{6}$$

376   Where [carbonyl], [CO] and [O_3] represented the observed mixing ratios of

377 carbonyl compounds, CO and ozone, respectively, in ppbv. β_0, β_1 and β_2 were

378 coefficients obtained by multiple linear regression fitting model, in ppbv/ppbv. β_0

379 represented the background concentration of a given carbonyl compound, β_1

380 represented the emission ratio of the carbonyl compound relative to CO. $\beta_1[CO]$ and

$\beta_2[O_3]$ represented the concentrations of carbonyl compound in primary emission and secondary formation, respectively, in ppbv.

In addition, the relative contribution of primary emissions, secondary formation and background concentrations of carbonyl compounds can be calculated using the following formula:

$$P_{primary} = \frac{\beta_1[CO]_i}{(\beta_0 + \beta_1[CO]_i + \beta_2[O_3]_i)} \times 100\% \qquad (7)$$

$$P_{secondary} = \frac{\beta_2[O_3]_i}{(\beta_0 + \beta_1[CO]_i + \beta_2[O_3]_i)} \times 100\% \qquad (8)$$

$$P_{background} = \frac{\beta_0}{(\beta_0 + \beta_1[CO]_i + \beta_2[O_3]_i)} \times 100\% \qquad (9)$$

Where, $P_{primary}$ represented the contribution of the primary emission of a given carbonyl compound, %; $P_{secondary}$ represented the contribution of the secondary formation of the carbonyl compound species, %; $P_{background}$ represented the contribution of the carbonyl compounds species from sources other than primary emissions and secondary formation, %.

(2) Backward trajectory model

The effects of long-distance air mass transport on the pollution of carbonyl compounds in the CPUA were studied using MeteoInfo software and TrajStat plug-in (http://www.meteothink.org/downloads/index.html).In this model, meteorological data were relevant meteorological data from the global date assimilation system (GDAS) database (ftp://arlftp.arlhq.noaa.gov/pub/archives/gdasl). A trajectory simulation height of 500 m above ground level (AGL) was selected. The duration of backward trajectory was 48 h. The daily start time was 00:00 UTC. The analog frequency was 2 h. The backward trajectory diagram was calculated. Meanwhile, the clustering method in TrajStat software and the Euclidean distance algorithm were used to cluster the airflow trajectory to the CPUA. And then the statistical analysis was carried out in combination with the corresponding pollutant mass concentration characteristics.

3. Results and Discussion

3.1 Overview of air quality during observation period

Due to the influence of cooling and precipitation caused by cold air intrusion, the early observation period (from August 4th to 6th, 2019) in the Chengdu Plain Urban Agglomeration (CPUA) experienced slightly lower temperatures (25.1°C) and higher humidity (87.6%). These conditions were unfavorable for ozone formation. Although ozone itself is not easily removed by rain, precipitation reduces ozone pollution by washing away its precursors, such as nitrogen oxides (NOx) and polar volatile organic compounds (VOCs), such as aldehydes, ketones, and others, decreasing sunlight exposure, and enhancing atmospheric dispersion. However, as temperatures increased and humidity dropped in the subsequent days, more favorable conditions for ozone formation emerged, leading to heavy and persistent regional ozone pollution in the CPUA. By August 12th, the mean temperature had gradually increased to 29.1°C, while it averaged 27.7°C from August 13th to 14th. During this time, cumulative precipitation reached 975 mm, resulting in temporary alleviation of ozone pollution. Subsequently, temperatures rose again from August 15th to 18th, with the mean temperature persisting above 28.4°C for several days, accompanied by a decrease in humidity to a minimum of 64.8% on August 17th. Overall, during the observation period (from August 4th, 2019, 0:00 to August 18th, 2019, 24:00), three episodes of severe ozone pollution occurred, namely EP1 (August 7th to 9th), EP2 (August 10th to 13th), and EP3 (August 15th to 18th), as depicted in Fig. 2.

Fig.3 illustrates the temporal and spatial variations of ozone and NO_2 concentrations, as well as temperature and humidity at each site during the observation period. After observing the spatial distribution of ozone concentration during EP1, it's evident that the severity of pollution reached heavily polluted levels, with Chengdu recording an MDA8 concentration of 297 $\mu g \cdot m^{-3}$ on August 7th. This distribution demonstrated a radial decrease from Chengdu to the surrounding areas. However, the subsequent episodes, EP2 and EP3, exhibited even broader ranges of ozone pollution and more pronounced spatial movements. During the early stages of EP2 and EP3 (from

435 August 10th to 11th and from August 14th to 15th, respectively), high ozone

436 concentrations were observed in the Chengdu-Deyang-Mianyang region. In the middle

437 stages (August 12th and from August 16th to 17th, respectively), influenced by northerly

438 airflow, regions with high ozone concentrations expanded to the central (Meishan,

439 Ziyang, and Suining) and southwestern (Leshan and Ya'an) parts of the CPUA. In the

440 later stages (August 13th and August 18th), under the influence of northwesterly airflow,

441 regions with high ozone concentrations (Meishan and Leshan) moved southward again,

442 while ozone pollution in other areas of the CPUA gradually weakened. On August 11th

443 to 12th and August 16th to 17th, ozone concentrations in the eight cities of the CPUA

444 reached light pollution levels or higher, with the heaviest pollution recorded on August

445 12th. Specifically, Deyang, Mianyang, Suining, and Meishan reached moderate

446 pollution levels, while Chengdu reached heavy pollution with a concentration of 324

447 $\mu g \cdot m^{-3}$.
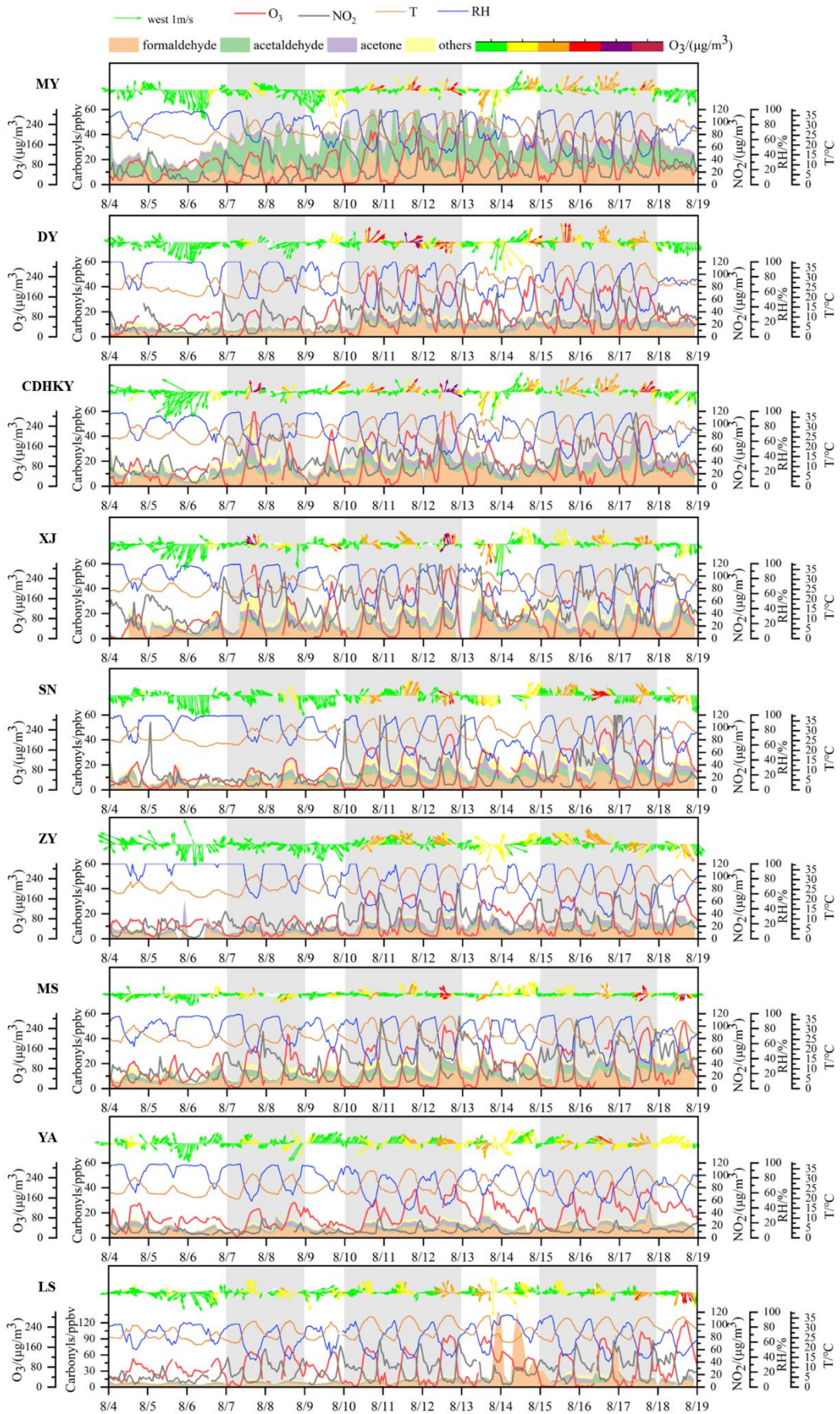
448
449 **Figure 2.** Overview of air quality at each site during the observation period. The gray shaded parts

450   respectively represent the three heavy ozone pollution episodes (EP1, EP2,EP3).
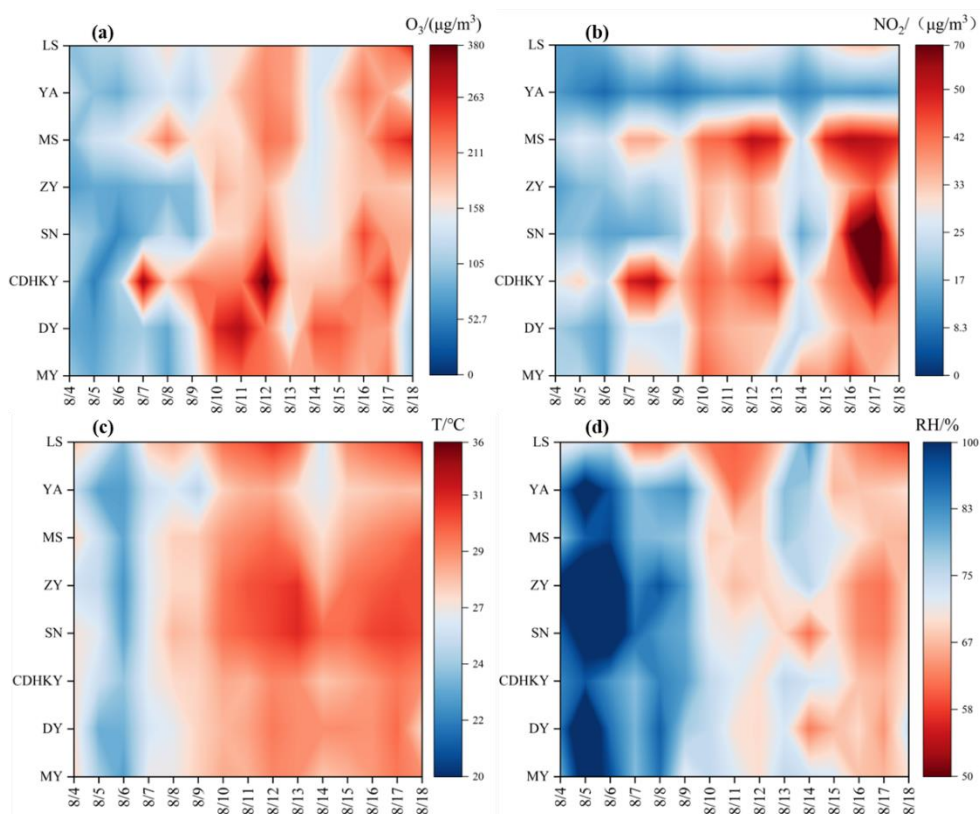
451

452 **Figure 3.** Temporal and spatial variations of (a) ozone concentration, (b) NO$_2$ concentration, (c)

453   temperature and (d) humidity in the CPUA during the observation period.

454 **3.2 Comparative characterization of carbonyl compounds**

455 **3.2.1 Ambient levels**

456   During the observation period, we utilized 2,4dinitrophenylhydrazine (DNPH)

457 cartridge and high-performance liquid chromatography (HPLC) analysis technique to

458 quantify 15 carbonyl compounds. The concentrations and relative proportions of these

459 compounds are summarized in Table 1. The average total concentration of the 15

460 carbonyls in the CPUA was 17.4 ± 5.3 ppb. Overall, areas with elevated concentrations

461 of carbonyl compounds were primarily concentrated in and around Chengdu in both

462 northern and southern directions. MY site, located to the north of Chengdu, exhibited

463 the highest concentration of carbonyl compounds (35.2 ± 13.4 ppb), while YA site,

464 situated southwest of Chengdu, showed the lowest concentration (10.7 ± 4.2 ppb).

465

466   **Table 1.** Daily mean ± standard error of carbonyl compound mixing ratios (ppbv) at each site in

467   the CPUA during the observation period. Sum: the total sum of carbonyl compound mixing ratios

468   across all compounds at each site.

Carbonyls	MY	DY	CDHKY	XJ	SN	ZY	MS	YA	LS
formaldehyde	12.8±6.5	6.1±2.8	10.1±4.2	8.9±4.4	7.0±3.6	5.8±2.7	8.5±4.2	6.4±2.4	6.6±3.4
acetaldehyde	16.7±7.4	1.5±0.8	3.7±2.2	2.3±1.1	2.6±1.7	1.4±0.6	3.2±1.6	0.9±0.7	1.6±1.3
acetone	4.4±1.7	2.8±1.2	4.5±2.3	3.7±1.2	3.1±1.7	3.2±1.7	2.2±1.1	2.2±1.1	2.9±1.6
propionaldehyde	0.4±0.2	0.2±0.1	0.4±0.3	0.4±0.2	0.3±0.2	0.3±0.1	0.4±0.2	0.2±0.12	0.3±0.2
crotoraldehyde	0.2±0.2	0.1±0.1	0.2±0.3	0.1±0.1	0.2±0.1	0.2±0.3	0.2±0.2	0.4±0.2	0.1±0.2
butyaldehyde	0.2±0.5	0.2±0.3	0.4±0.6	0.9±1.7	0.3±0.2	0.1±0.2	0.4±0.5	0.3±0.2	0.0±0.1
benzaldehyde	0.0±0.0	0.0±0.1	0.0±0.1	0.2±0.2	0.1±0.1	0.0±0.0	0.0±0.0	0.0±0.0	0.0±0.0
isovaleraldehyde	0.0±0.1	0.0±0.1	0.1±0.1	0.1±0.1	0.1±0.1	0.0±0.1	0.7±0.4	0.0±0.1	0.1±0.1
valeraldehyde	0.0±0.0	0.3±0.1	0.3±0.6	0.6±0.4	0.9±0.7	0.0±0.0	0.0±0.0	0.0±0.0	0.8±0.5
o-Tolualdehyde	0.5±0.5	0.4±0.3	0.5±0.2	0.0±0.0	0.0±0.0	0.2±0.2	0.4±0.3	0.2±0.2	0.2±0.2
m-Tolualdehyde	0.0±0.0	0.0±0.1	0.0±0.1	0.2±0.2	0.3±0.1	0.0±0.0	0.0±0.0	0.0±0.0	0.0±0.1
p-Tolualdehyde	0.0±0.0	0.0±0.1	0.0±0.0	0.0±0.0	0.0±0.0	0.0±0.0	0.0±0.0	0.0±0.0	0.0±0.0
hexaldehyde	0.0±0.0	0.3±0.3	0.4±0.7	0.6±0.5	1.0±0.7	0.0±0.2	0.8±0.6	0.0±0.0	0.1±0.3
2,5-diemthybenzaldehyde	0.0±0.0	0.0±0.0	0.0±0.0	0.1±0.1	0.0±0.0	0.0±0.0	0.0±0.0	0.0±0.0	0.0±0.0
MACR	0.0±0.2	0.1±0.2	0.3±0.3	1.1±1.1	0.3±0.2	0.2±0.2	0.4±0.4	0.2±0.2	0.8±0.9
Sum	35.2±13.4	12.2±4.8	20.8±8.9	19.0±8.1	16.1±7.7	11.5±4.9	17.2±7.6	10.7±4.2	13.5±6.1

469

470

471

Fig.S1 illustrates the relationship between ozone concentration and carbonyl compounds concentration at each site during the observation period. It is evident that the spatial distribution of carbonyl compound concentrations is similar to that of ozone concentration. Regions with severe ozone pollution tend to exhibit higher concentrations of carbonyl compounds. The variation in carbonyl compound concentrations is primarily attributed to anthropogenic emissions and prevailing summer wind directions in the CPUA. Chengdu is the most economically developed city in the CPUA, with notably higher GDP and industrial production values than other regions. Chengdu's major industries include coal-fired power plants, chemical plants, metallurgy and building materials plants, and high concentrations of carbonyls were observed in here. The unique basin climate of the CPUA, characterized by intense sunlight and stable atmospheric conditions, facilitates the accumulation of pollutants. Large amount of industrial emissions and strong photochemical reaction contributes to ozone pollution. Additionally, during the summer, prevailing northerly winds in the CPUA facilitate the downwind transport of pollutants from upwind sources, leading to regional pollution. It is noteworthy that the concentration of carbonyl compounds at the MY site significantly exceeds that at the CDHKY site. Mianyang, with its industrial roots, consistently maintains its position as the second-highest GDP contributor in Sichuan Province. The electronics information industry stands as Mianyang's primary economic driver, constituting approximately half of the city's total output value. Studies investigating the volatile organic compound (VOC) source profile in Chengdu(Zhou et al., 2021) reveal that ethanol and carbonyls predominantly characterize electronics manufacturing emissions.

3.2.2 Compositional characteristics

According to the composition characteristics of 15 carbonyl compounds in the ambient air of each city during the observation period(Table S4).Formaldehyde was

498   the most abundant carbonyl found in these sites followed by acetone and acetaldehyde,

499   which is widely observed in previous studies. The measured ratios of formaldehyde,

500   acetone, and acetaldehyde across different sites ranged from 36.4% to 59.4% (average

501   48.1%), 12.4% to 28.1% (average 19.9%), and 8.2% to 47.3% (average 17.5%),

502   respectively. In this study, the total measured of formaldehyde, acetaldehyde, and

503   acetone(FAT)account for over 78% of the total carbonyls concentrations. At the MY

504   and ZY sites, this proportion even exceeded 90%. It is noteworthy that isobutyraldehyde

505   (MACR) ranks fourth in the volume concentration of 15 carbonyls measured in the

506   ambient air surrounding XJ, accounting for 5.3%. MACR, a characteristic product of

507   isoprene photooxidation from biogenic sources, possibly originates from the abundant

508   vegetation surrounding XJ. It reflects the period's relatively active photochemical

509   reactions, with substantial contributions from secondary formation to the measured

510   carbonyls composition.

511   The observed levels of FAT in different areas were influenced by various factors

512   including sampling period, geographic location, meteorological conditions, chemical

513   removal, and source emissions(Z. Zhang et al., 2016). Despite these influences,

514   comparisons remain valuable in providing an overview of ambient carbonyl levels in

515   the CPUA. During the summer of 2010, a national wide survey of ambient

516   monocarbonyl compounds were conducted simultaneously in nine sites (Ho et al.,

517   2015)found that the total FAT concentration was highest in Chengdu (14.96 ppb),

518   followed by Beijing (11.83 ppb), and Wuhan (11.70 ppb). Beijing, as the capital of

519   China, and Wuhan, being one of the top ten most populous cities in China, played

520   significant roles in this comparison. In our study, the CDHKY site within CPUA

521   exhibited the highest FAT concentration, with values of 18.25 ppb, surpassing those

522   recorded in 2010. Furthermore, the total FAT concentrations observed at the CPUA and

523   XJ sites, with values of 14.99 ppb and 14.90 ppb respectively in our study, closely

524   resemble those reported in August 2010 in Chengdu. The consistently high levels of

525   carbonyl compounds observed in Chengdu, both in 2010 and our current study, indicate

526   that the city likely experiences higher concentrations of these pollutants compared to

527   other regions across the country. However, more extensive temporal data would be

528   beneficial to fully validate this pattern at a national scale. Comparing our findings to

529   international studies, the FAT concentrations at the CDHKY site were lower than those

530   reported in Rio De Janeiro, Brazil(da Silva et al., 2016), during July to October 2013

531   (35.43 ppb), but higher than those in Bangkok, Thailand(Kanjanasiranont et al., 2016b),

532   Orleans, France(Jiang et al., 2016), and the United States(Murillo et al., 2012), with

533   values of 9.05 ppb, 6.12 ppb, and 5.76 ppb, respectively.

534   **3.3 Temporal variations of carbonyl compounds**

535   The diurnal variation of the total mixing ratio of ambient carbonyl compounds and

536   ozone concentration around each site in the CPUA during the observation period is

537   shown in Fig. 4. According to the observation results, the diurnal trend of ozone

538   concentration at each site showed a "unimodal" variation characteristic, that was, it

539   gradually increased from the morning to the peak of one day at noon, and then decreased.

540   The diurnal variation of the total mixing ratio of carbonyl compounds at each site

541   generally showed a characteristic of high during the daytime and low at night. The

542   concentration of carbonyl compounds during the day (6:00-16:00) was 48.8% higher

543   than that at night (18:00-4:00) at the XJ site. This indicated that the concentration of

544   carbonyl compounds increased by photochemical production during the daytime.

545   Additionally, deposition processes, particularly dry deposition at night, likely

546   contribute to the observed diurnal variation in carbonyl levels. The diurnal variation

547   characteristics of each site were different. For example, the diurnal variation

548   characteristics of carbonyl compounds concentration at CDHKY, XJ and SN sites were

549   consistent with those of ozone. The diurnal variation of carbonyl compounds

550   concentrations at other sites showed "double peaks", peaking at 10:00-12:00 and 18:00-

551   20:00, respectively. The concentrations of carbonyl compounds at night were also

552   higher at MY, DY and LS sites. The diurnal minimum values of the total concentration

553   of carbonyl compounds and ozone concentration appeared at similar time, usually at

554 4:00 a.m. or 6:00 a.m. The first peak of the total mixing ratio of carbonyl compounds

555 occurred earlier than the maximum ozone concentration of the day. The first peak of

556 the total mixing ratio of carbonyl compounds mostly occurred between 10:00 and 12:00.

557 And the maximum ozone concentration mostly occurs between 14:00 and 16:00. This

558 was related to the fact that carbonyl compounds were important precursors of ozone.

559   In general, the diurnal variation of the total concentration of carbonyl

560 compounds on pollution days and clean days was high during the daytime and low at

561 night. The total mixing ratio of carbonyl compounds on pollution days was 22.8%-

562 66.2% higher than that on clean days. At the same time, the increase of concentration

563 of carbonyl compounds during the daytime on pollution days was higher than that on

564 clean days. This suggested that the increase in the concentration of carbonyl

565 compounds during the daytime contributed to ozone pollution.
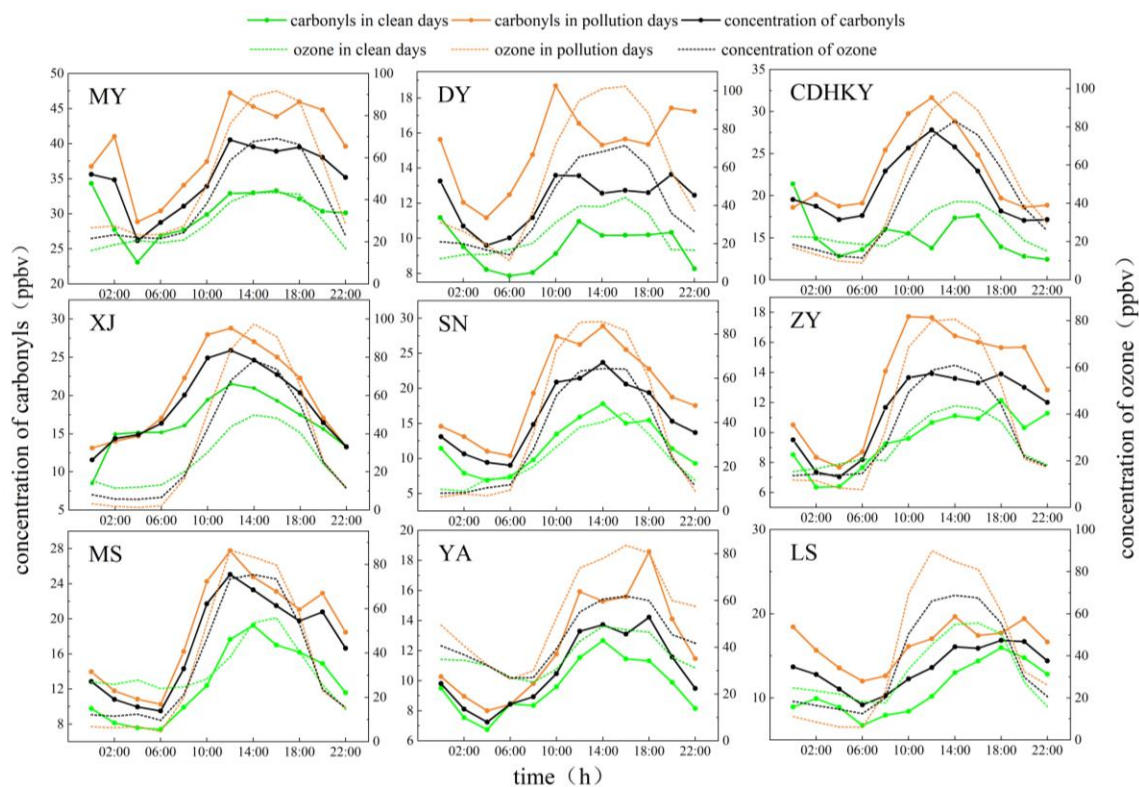
566

567 **Figure 4.** Diurnal variations of carbonyl compounds and ozone concentrations at each site in the

568   CPUA during the observation period

569 **3.4 Atmospheric photochemical reactivity of carbonyl compounds**

570   During the observation period, the total OH radical consumption rate (L_{OH}) and

571   total ozone formation potential (OFP) of the 15 carbonyl compounds at each site are

572   depicted in Fig.5. The ranking of total L_{OH} and total OFP at each site is consistent,

573   except for the YA and ZY sites with lower concentrations of carbonyl compounds,

574   where the atmospheric photochemical reactivity ranking also aligns with the

575   concentration. Among all sites, the MY and CD sites display the highest reactivity,

576   while the YA and ZY sites exhibit the lowest reactivity. During the observation period,

577   carbonyl compounds significantly contributed to ozone formation. The contributions to

578   total VOCs (alkanes, alkenes, alkynes, aromatics, and carbonyl compounds) OFP at the

579   MY, SN, ZY, YA, and LS sites ranged from 19.5% to 48.6%. Formaldehyde and

580   acetaldehyde were identified as the most reactive species in the atmosphere, surpassing

581   other carbonyl compounds in reactivity due to their higher concentrations and inherent

582   reactivity, especially formaldehyde. However, acetone exhibited high inertness and a

583   prolonged atmospheric lifetime, leading to its accumulation in ambient air with

584   concentrations higher than other carbonyl compounds except for formaldehyde and

585   acetaldehyde. Thus, despite its elevated concentration, acetone's reactivity remained

586   relatively low.
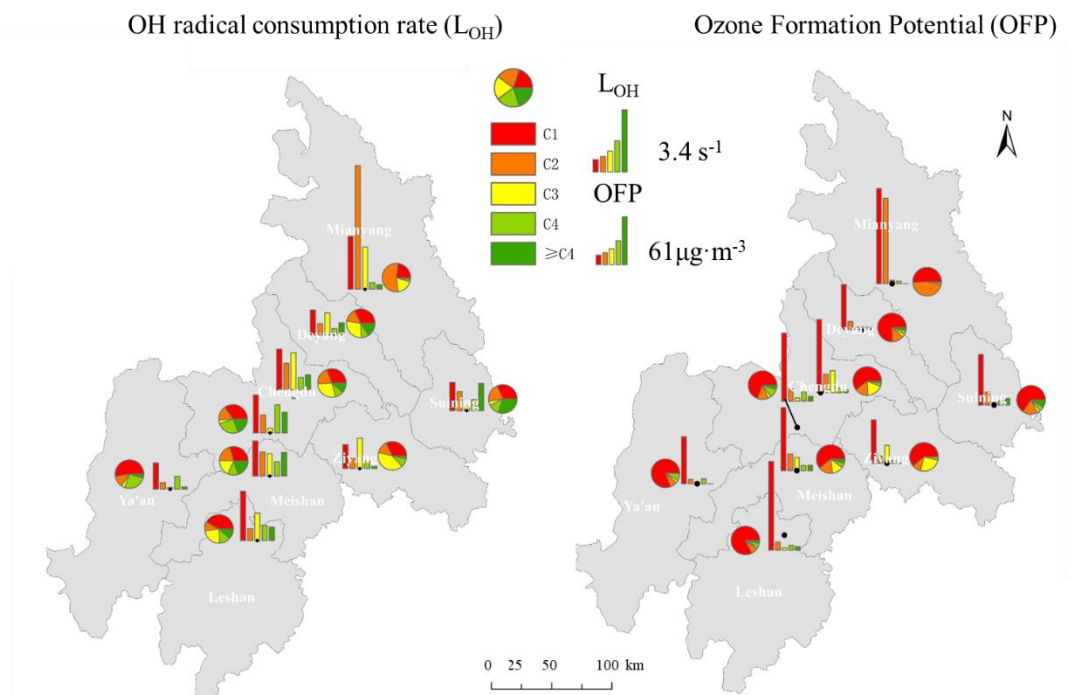
587

588   **Figure 5.** L_{OH} and OFP of carbonyl compounds at each site in the CPUA during the observation

589   period

590   3.5 Sensitivity analysis of ozone formation based on formaldehyde to NO₂ ratio (FNR)

591   The change of O_3 formation sensitivity of each site in the CPUA during the

592   observation period is shown in Fig.6. As can be seen from the Fig. 6, most sites remain

593   in the VOCs-limited regime during the cleaning period and EP1 to EP3. Economically

594   developed city such as Chengdu, Meishan, with high levels of formaldehyde and NO_2,

595   remain in the VOCs-limited regime. Ya'an as a city with the lowest GDP ranking in the

596   CPUA, with low levels of formaldehyde and NO_2, remain in the transitional regime.
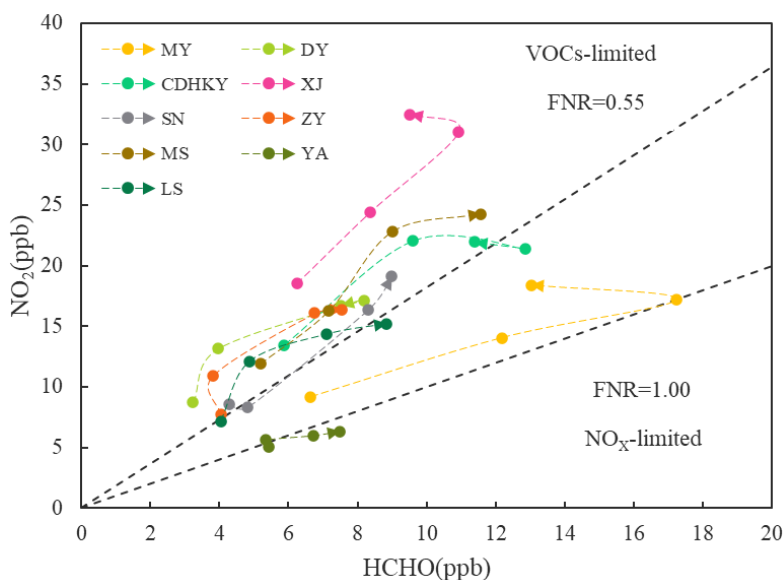
597

598   Figure 6. The change of O_3 formation sensitivity of each site in the CPUA during the observation

599   period. The arrows represent time step from clean period to EP1 to EP2 to EP3.

600   The daily variation of O_3 formation sensitivity and ozone concentration at each

601   site in the CPUA during the observation period is shown in Fig. S4. The mean FNR of

602   each site ranged from 0.48 to 1.29 during the observation period. The FNRs were lower

603   than 0.55±0.16 at XJ, DY, ZY, CDHKY, and MS, and higher than 1.0 at LS, SN, YA

604   and MY. At the same time, the mean ozone concentration at each site was between 138

605   and 192 µg·m⁻³. The mean ozone concentration in XJ, DY, CDHKY and MS was 166-

606   192 µg·m⁻³, it was 150-164 µg·m⁻³ in LS, SN, YA and MY. Therefore, it could be seen

607   that most of the sites with high mean ozone concentrations during the observation

period, like CDHKY, XJ, MS and Deyan sites, were in the VOCs-limited regime, and most of the stations with low mean ozone concentrations during the observation period such as YA, SN, MY and LS were in the transitional regime. It was worth noting that the mean ozone concentration at ZY site (only 138 $\mu g \cdot m^{-3}$) during the observation period was much lower than that of other sites, but most of the ZY site was in VOCs-limited regime, which was mainly related to the low concentration of formaldehyde. In addition, the FNR value of the MY site was also relatively high, which was mainly caused by the high concentration of formaldehyde.

Based on the ratio of formaldehyde to NO_2 mixing ratio, most sites remain in the VOCs-limited regime during the observation period. And the sites with heavy ozone pollution were in the VOCs-limited regime, and the sites with light ozone pollution were in the transitional regime. Photochemical reactivity (L_{OH} and OFP) analysis showed that formaldehyde and acetaldehyde contributed significantly to the enhancement of atmospheric oxidation and ozone formation potential. Therefore, when heavy ozone pollution occurs in the CPUA, special attention should be paid to the control of VOCs, especially formaldehyde and acetaldehyde in carbonyl compounds, under the coordinated control of NOx and VOCs. Overall, this study reveals the important contribution of carbonyl compounds to ozone pollution in the CPUA, and provides scientific support for the establishment of ozone pollution prevention and control measures.

3.6 Source Analysis of carbonyl compounds

3.6.1 Quantitative source analysis of key carbonyl compounds

The table S7 provides a summary of the background and primary emissions concentrations of formaldehyde, acetaldehyde, and acetone at nine sites across the eight cities of the CPUA, along with the proportion of secondary formation contributing to their concentrations. Background concentrations and primary emissions of formaldehyde, acetaldehyde, and acetone ranged from 50% to 80%, 46% to 83%, and

635   45% to 78%, respectively. Secondary formation accounted for 20% to 50%, 17% to

636   54%, and 22% to 55% of their concentrations, respectively. Notably, in SN and YA, the

637   secondary formation of formaldehyde contributed half of the observed concentration,

638   indicating it as the predominant source, while acetaldehyde's secondary formation also

639   prevailed in these sites. Conversely, acetone, with lower reactivity, primarily originated

640   from background concentrations and primary emissions at other sites except YA.

641   Moreover, background concentrations and primary emissions were identified as the

642   main contributors to carbonyl compounds in XJ and LS.

643   Fig.7 illustrates the secondary formation concentrations of formaldehyde,

644   acetaldehyde, and acetone at each site in the CPUA under both clean and polluted

645   conditions. Under polluted conditions, the secondary concentrations of formaldehyde,

646   acetaldehyde, and acetone exceeded those in clean conditions by 58.8%, 54.6%, and

647   57.6%, respectively. The most significant increases in secondary concentrations were

648   observed at the SN site, while relatively smaller increases were observed at LS and XJ.
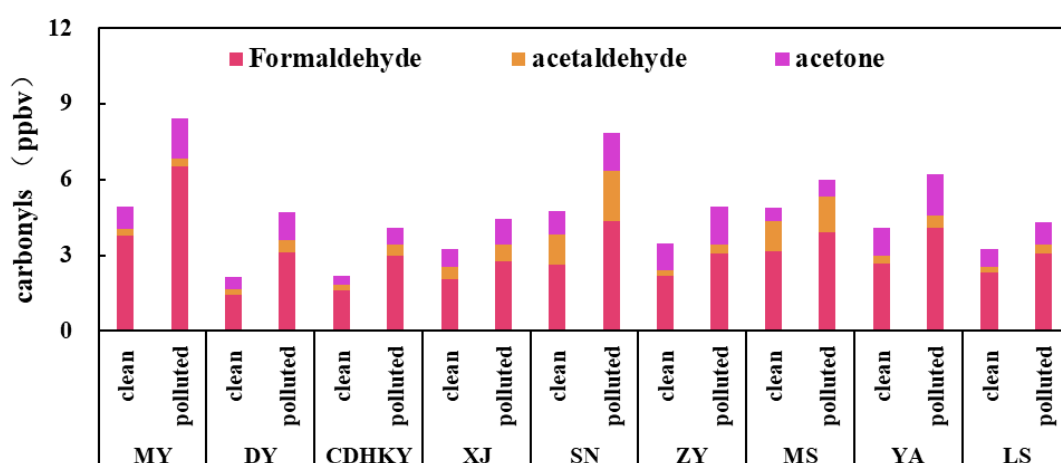
650   **Figure 7.** Concentrations of formaldehyde, acetaldehyde and acetone in secondary formation

651   under different pollution conditions at each site in the CPUA during the observation period

652   **3.6.2 Exploration of secondary formation mechanism of key carbonyl compounds**

653   In this study, we utilized VOC data collected on August 11, 12, and 16, when all

654   eight cities in the CPUA were experiencing mild to severe ozone pollution. We

655   calculated the Relative Incremental Reactivity (RIR) of formaldehyde, acetaldehyde,

656 and acetone at the MY, SN, ZY, YA, and LS sites on these days. The OBM analysis

657 allowed us to assess the impact of anthropogenic VOCs (alkanes, alkenes, alkynes,

658 aromatics) and biogenic VOCs (e.g., isoprene) on carbonyl compound formation in the

659 context of regional ozone pollution events (Fig.8). Overall, the sensitivities of different

660 anthropogenic source and plant source VOCs to formaldehyde, acetaldehyde and

661 acetone was consistent among sites. For formaldehyde, reducing alkenes in

662 anthropogenic source VOCs and plant VOCs was the most effective way to control

663 formaldehyde concentration, while reducing alkenes in anthropogenic source VOCs

664 was also beneficial to reduce the formation of acetaldehyde. For acetone with low

665 reactivity, the alkanes in anthropogenic source VOCs were the most sensitive to the

666 formation of acetone, followed by alkenes and BVOCs. Only the RIR value of alkanes

667 were greater than zero, and the RIR values of both alkenes and BVOCs were less than

668 zero, indicating that reducing alkanes could reduce the formation of acetone, while

669 reducing alkenes and BVOCs was not conducive to acetone concentration control.
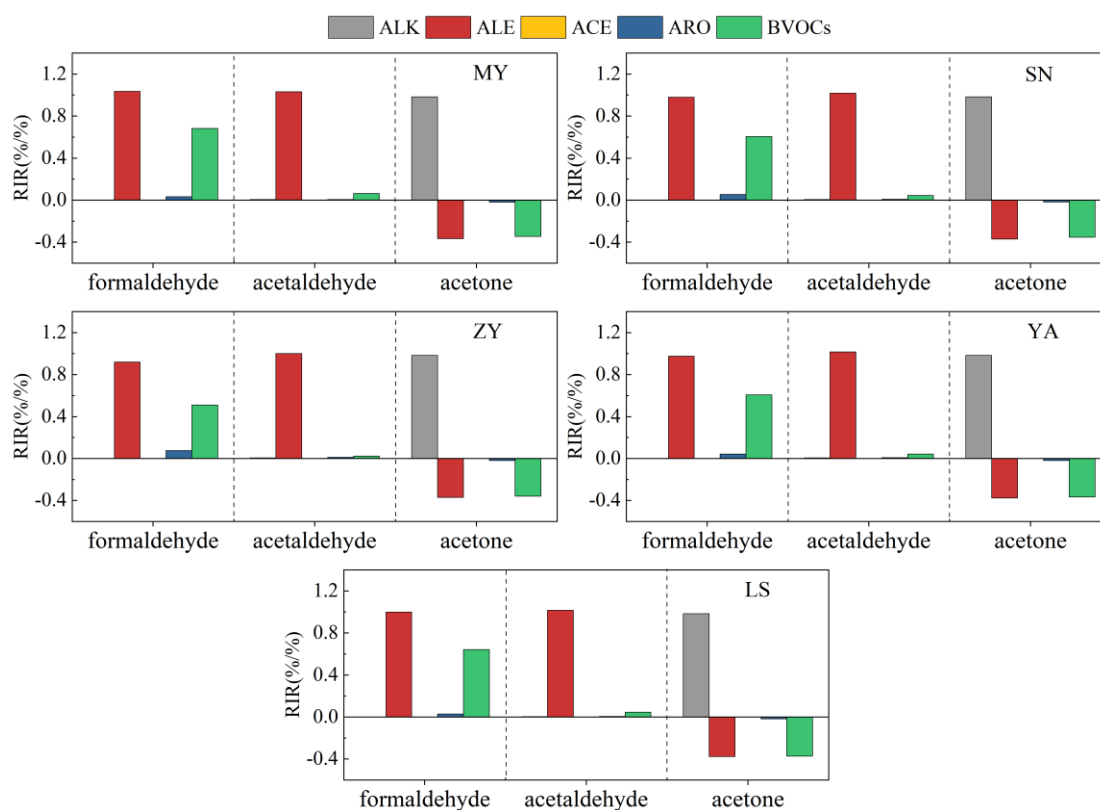
670

671 **Figure 8.** Mean RIRs of formaldehyde, acetaldehyde and acetone to different anthropogenic

672 source VOCs (alkanes (ALK), alkenes (ALE), alkynes(ACE), aromatics (ARO))and biogenic

673   VOCs (BVOCs)at MY, SN, ZY, YA and LS sites on August 11th, 12th and 16th.

3.6.3 Influence of regional transportation contribution

674

675   The TrajStat trajectory model was used to calculate and cluster the 24-hour

676 backward trajectories of air quality at the sampling sites. The backward trajectory

677 during sampling is shown in Fig.S5. During the observation period, the pollution of

678 carbonyl compounds in the cities of the CPUA was affected by the mutual transport

679 among cities in Sichuan Province, especially along the MY-DY-CDHKY route. In

680 addition, the surrounding provinces and cities of Sichuan Province (Gansu and

681 Chongqing) also contributed to the carbonyl compounds of the CPUA.

682   The potential sources of carbonyl compounds at different pollution stages at the

683 CDHKY during the observation period are shown in Fig. 9. It can be seen from the

684 figure that there are differences in the potential sources of carbonyl compounds among

685 different pollution stages at the CDHKY site. The concentration of local carbonyl

686 compounds in CDHKY was high during the early observation period and EP1, which

687 existed local sources, and was also affected by the northern airflow, and carbonyl

688 compounds was also affected by the transport from MY, DY and other northern regions.

689 Under the effect of the continuous northern airflow, the local source emissions

690 decreased during EP1, and the potential source of carbonyl compounds changed to from

691 the junction between CDHKY and ZY. During EP3, under the combined influence of

692 the western airflow, the contribution of transport from SN and ZY to carbonyl

693 compounds increased, while emissions from local sources also increased.
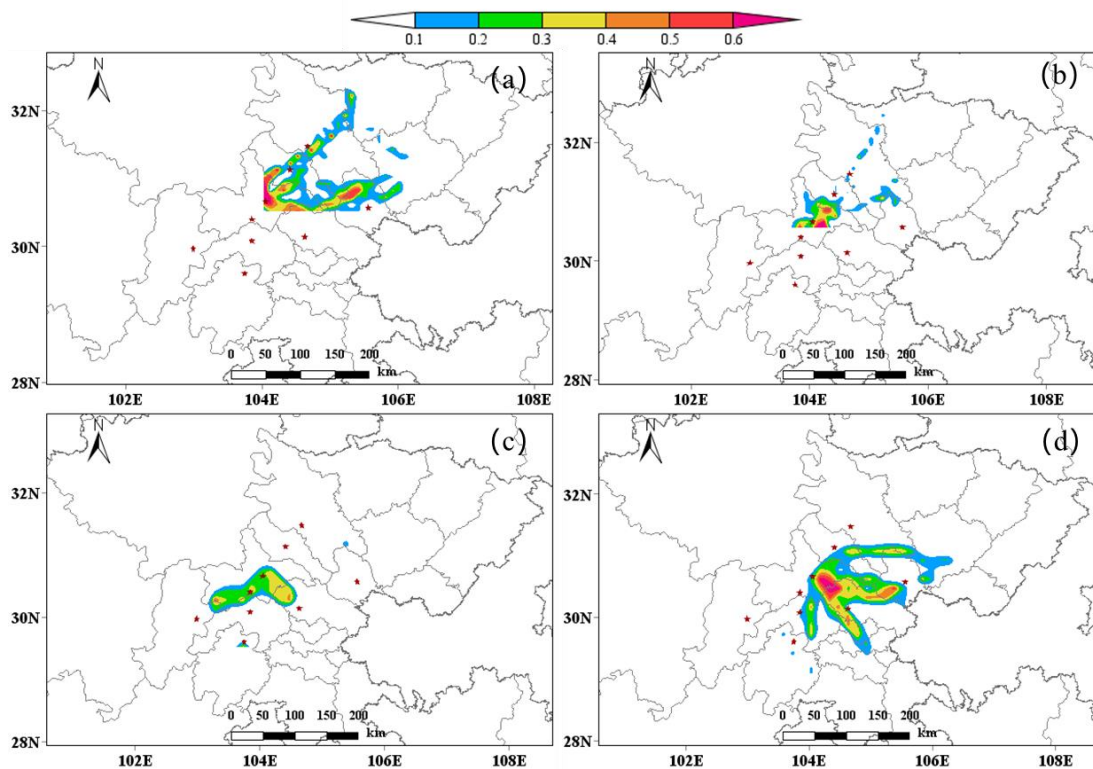
Figure 9. Analysis of potential sources of carbonyl compounds at different periods at the CDHKY site during the observation period (a) August 4th-6th (b) August 7th-9th (c) August 10th-13th (d) August 15th-18th

4. Conclusions

During a comprehensive atmospheric observation campaign conducted at nine sites across the CPUA from August 4th to 18th, 2019, three regional heavy ozone pollution episodes(EP1 to EP3) were observed. This study extensively examines the concentration variations, atmospheric chemical reactivity, and sources of carbonyls during this period. The average total concentrations of 15 carbonyl compounds across the nine sites within eight cities of the CPUA were measured at 17.4 ± 5.3 ppb. Spatial analysis indicated that areas with higher carbonyl concentrations were concentrated around Chengdu, extending both north and south. Notably, regions with elevated carbonyl compound concentrations also tended to experience more severe ozone pollution. Formaldehyde (36.4%-64.3%), acetone (12.4%-28.1%), and acetaldehyde (8.2%-47.3%) constituted the predominant species by volume concentration. Chengdu

710   exhibited FAT concentrations surpassing national and international levels, indicating

711   heightened levels compared to other regions.

712   Compared to clean days, carbonyl compound concentrations were significantly

713   higher on ozone pollution days, with increases ranging from 22.8% to 66.2%. Between

714   19.5% and 48.6% of the total volatile organic compound (VOC) ozone formation

715   potential (OFP) was attributed to the 15 carbonyl compounds, highlighting their

716   substantial contribution to ozone formation, particularly formaldehyde and

717   acetaldehyde. While primary emissions are the main sources of these compounds,

718   secondary formation processes contributed over 30% on average to the concentrations

719   of formaldehyde, acetaldehyde, and acetone. Under ozone pollution conditions, the

720   secondary formation concentrations of these three compounds were notably higher than

721   on clean days, with increases of 58.8%, 54.6%, and 57.6%, respectively, emphasizing

722   the critical role of secondary processes in exacerbating regional ozone pollution. OBM

723   modeling revealed that formaldehyde and acetaldehyde primarily originated from the

724   secondary formation of alkenes and BVOCs, while acetone mainly stemmed from the

725   secondary formation of alkanes. These findings highlight that while the concentration

726   of carbonyl compounds is important, their significant impact on ozone formation is

727   primarily driven by secondary chemistry. Specifically, the secondary formation of these

728   compounds from alkenes and biogenic BVOCs plays a key role in this process.

729   Ground-level observations of the formaldehyde to NO_2 ratio (FNR) were utilized

730   to assess the sensitivity of ground-level ozone formation. Analysis of FNR revealed that

731   sites experiencing heavy ozone pollution exhibited lower FNRs, indicating a VOCs-

732   limited regime, while sites with lighter ozone pollution were categorized into a

733   transitional regime. Furthermore, it is recommended to establish a scientific control

734   mechanism for both NOx and VOCs, with special attention to formaldehyde,

735   acetaldehyde, and acetone, and their alkenes precursors. Additionally, considering the

736   regional nature of pollution, this study suggests that carbonyl compound pollution is

737   influenced by mutual transport among cities within the CPUA, notably along the MY-

DY-CDHKY route. Establishing a collaborative prevention and control mechanism among cities within the CPUA and neighboring provinces and cities is crucial to effectively address carbonyl compounds and ozone pollution in the region in the future.

Data availability. Observational data including meteorological parameters and air pollutants used in this study are available from the corresponding authors upon request (lihong@craes.org.cn).

Author contributions. Hong Li and Jiemeng Bao designed this study. Xin Zhang, Zhenhai Wu, Jiemeng Bao, Li Zhou, Qinwen Tan, and Fumo Yang coordinated the selection of field observation sites, including locations for both VOCs and carbonyls grid sampling. Qinwen Tan and Hefan Liu supported the collection of carbonyls at one site. Zhenhai Wu and Xin Zhang assisted in carbonyls sampling; Xin Zhang and Yunfeng Li assisted in carbonyls sample analysis and data collection. Li Zhou and Hefan Liu organized the analysis of VOCs measurements. Jun Qian, Junhui Chen, and Liqun Deng provided support in project funding application. Jiemeng Bao performed the data analysis and wrote the paper with contributions from all co-authors; Hong Li reviewed the paper, provided comments and finalized it.

Competing interests. The contact author has declared that none of the authors has any competing interests.

Acknowledgments. The authors would like to express their sincere appreciation to Keding Lu and Xin Li of Peking University for their organization of the intensive field observation experiment on the formation mechanisms of photochemical pollution in summer in the CPUA of China. They also want to show their deep gratitude to Yulei Ma, Tianli Song, Xiaodong Wu, Ning Wang, and He Zijun Liu of Sichuan University, as well as Xin Zhang (female) and Hefan Liu of Chengdu Academy of Environmental

766 Protection Sciences for their help in sampling. They are also grateful to Liping Liu of

767 Sichuan Agricultural University in Ya'an City, Kaiyao Lv of Mianyang High-tech Zone

768 Management Committee, Yong Xiao of Deyang Municipal Education Bureau, Ying Ni

769 of Meishan Ecological Environment Bureau, Aihua Zou of Leshan Ecological

770 Environment Bureau, and Chuhan Wang of the Chinese Academy of Environmental

771 Sciences for their substantial support during field observations. Special thanks to Zhen

772 He and Manfei Yin of the Chinese Academy of Environmental Sciences for their

773 assistance in analyzing samples from the XJ site.

774

775 **Financial support.** This research has been supported by the Research Project on

776 Analysis of Multiple Causes of Atmospheric Ozone Pollution in Urban Agglomerations

777 of Chengdu Plain and Development of Management, Prevention, and Control System

778 of Sichuan Academy of Environmental Sciences (No. 510201201905430).

779

780 **References**

781 Altshuller, A. P. (1993). Atmospheric chemistry of VOCs and NOx: Implications for
782   ozone formation. *Environmental Science & Technology*, 27(6), 1104–1117.
783   doi:10.1021/es00043a001

784 Atkinson, R., Arey, J., 2003. Atmospheric Degradation of Volatile Organic Compounds.
785   Chem. Rev. 103, 4605–4638. https://doi.org/10.1021/cr0206420

786 Bao, J., Li, H., Wu, Z., Zhang, X., Zhang, H., Li, Y., Qian, J., Chen, J., Deng, L., 2022.
787   Atmospheric carbonyls in a heavy ozone pollution episode at a metropolis in
788   Southwest China: Characteristics, health risk assessment, sources analysis.
789   Journal of Environmental Sciences 113, 40–54.
790   https://doi.org/10.1016/j.jes.2021.05.029

791 Cardelino, C., Chameides, W., 1995. An observation-based model for analyzing ozone
792   precursor relationships in the urban atmosphere. J. Air Waste Manage. Assoc.
793   45, 161–180.

794 Coggon, M. M., Veres, P. R., Yuan, B., et al. (2019). Emissions of organic carbonyl
795   compounds from biomass burning: A global source of reactive carbon to the
796   atmosphere. *Environmental Science & Technology*, 53(20), 11401–11412.

797 da Silva, D.B.N., Martins, E.M., Corrêa, S.M., 2016. Role of carbonyls and aromatics
798   in the formation of tropospheric ozone in Rio de Janeiro, Brazil. Environ Monit
799   Assess 188, 289. https://doi.org/10.1007/s10661-016-5278-3

800   Duan, J., Guo, S., Tan, J., Wang, S., Chai, F., 2012. Characteristics of atmospheric
801   carbonyls during haze days in Beijing, China. Atmospheric Research 114–115,
802   17–27. https://doi.org/10.1016/j.atmosres.2012.05.010

803   Duan, J., Tan, J., Yang, L., Wu, S., Hao, J., 2008. Concentration, sources and ozone
804   formation potential of volatile organic compounds (VOCs) during ozone
805   episode in Beijing. Atmospheric Research 88, 25–35.
806   https://doi.org/10.1016/j.atmosres.2007.09.004

807   Fu, T.-M., Jacob, D.J., Wittrock, F., Burrows, J.P., Vrekoussis, M., Henze, D.K., 2008.
808   Global budgets of atmospheric glyoxal and methylglyoxal, and implications for
809   formation of secondary organic aerosols. Journal of Geophysical Research:
810   Atmospheres 113. https://doi.org/10.1029/2007JD009505

811   Fuchs, H., Tan, Z., Lu, K., Bohn, B., Broch, S., Brown, S.S., Dong, H., Gomm, S.,
812   Häseler, R., He, L., Hofzumahaus, A., Holland, F., Li, X., Liu, Y., Lu, S., Min,
813   K.-E., Rohrer, F., Shao, M., Wang, B., Wang, M., Wu, Y., Zeng, L., Zhang,
814   Yinson, Wahner, A., Zhang, Yuanhang, 2017. OH reactivity at a rural site
815   (Wangdu) in the North China Plain: contributions from OH reactants and
816   experimental OH budget. Atmospheric Chemistry and Physics 17, 645–661.
817   https://doi.org/10.5194/acp-17-645-2017

818   Grosjean, D., & Seinfeld, J. H. (1989). Parameterization of the formation potential of
819   secondary organic aerosols. *Atmospheric Environment*, 23(8), 1733–1747.
820   doi:10.1016/0004-6981(89)90058-9

821   Guo, H., Wang, T., Simpson, I.J., Blake, D.R., Yu, X.M., Kwok, Y.H., Li, Y.S., 2004.
822   Source contributions to ambient VOCs and CO at a rural site in eastern China.
823   Atmospheric Environment 38, 4551–4560.
824   https://doi.org/10.1016/j.atmosenv.2004.05.004

825   Hallquist, M., Wenger, J. C., Baltensperger, U., et al. (2009). The formation, properties,
826   and impact of secondary organic aerosol: Current and emerging issues.
827   *Atmospheric Chemistry and Physics*, 9, 5155–5236. doi:10.5194/acp-9-5155-
828   2009

829   Ho, K.F., Ho, S.S.H., Huang, R.-J., Dai, W.T., Cao, J.J., Tian, L., Deng, W.J., 2015.
830   Spatiotemporal distribution of carbonyl compounds in China. Environmental
831   Pollution 197, 316–324. https://doi.org/10.1016/j.envpol.2014.11.014

832   Hong, Q., Zhu, L., Xing, C., Hu, Q., Lin, H., Zhang, C., Zhao, C., Liu, T., Su, W., Liu,
833   C., 2022. Inferring vertical variability and diurnal evolution of O3 formation
834   sensitivity based on the vertical distribution of summertime HCHO and NO2 in
835   Guangzhou, China. Science of The Total Environment 827, 154045.
836   https://doi.org/10.1016/j.scitotenv.2022.154045

837   Hu, J., Wang, P., Ying, Q., Zhang, H., Chen, J., Ge, X., Li, X., Jiang, J., Wang, S., Zhang,
838   J., Zhao, Y., Zhang, Y., 2017. Modeling biogenic and anthropogenic secondary
839   organic aerosol in China. Atmospheric Chemistry and Physics 17, 77–92.
840   https://doi.org/10.5194/acp-17-77-2017

841   Jiang, Z., Grosselin, B., Daële, V., Mellouki, A., Mu, Y., 2016. Seasonal, diurnal and

842   nocturnal variations of carbonyl compounds in the semi-urban environment of
843   Orléans, France. Journal of Environmental Sciences, Changing Complexity of
844   Air Pollution 40, 84–91. https://doi.org/10.1016/j.jes.2015.11.016

845 Kanjanasiranont, N., Prueksasit, T., Morknoy, D., Tunsaringkarn, T., Sematong, S.,
846   Siriwong, W., Zapaung, K., Rungsiyothin, A., 2016a. Determination of ambient
847   air concentrations and personal exposure risk levels of outdoor workers to
848   carbonyl compounds and BTEX in the inner city of Bangkok, Thailand.
849   Atmospheric   Pollution   Research   7,   268–277.
850   https://doi.org/10.1016/j.apr.2015.10.008

851 Kanjanasiranont, N., Prueksasit, T., Morknoy, D., Tunsaringkarn, T., Sematong, S.,
852   Siriwong, W., Zapaung, K., Rungsiyothin, A., 2016b. Determination of ambient
853   air concentrations and personal exposure risk levels of outdoor workers to
854   carbonyl compounds and BTEX in the inner city of Bangkok, Thailand.
855   Atmospheric   Pollution   Research   7,   268–277.
856   https://doi.org/10.1016/j.apr.2015.10.008

857 Li, N., Fu, T.-M., Cao, J., Lee, S., Huang, X.-F., He, L.-Y., Ho, K.-F., Fu, J.S., Lam, Y.-
858   F., 2013. Sources of secondary organic aerosols in the Pearl River Delta region
859   in fall: Contributions from the aqueous reactive uptake of dicarbonyls.
860   Atmospheric Environment, Improving Regional Air Quality over the Pearl
861   River Delta and Hong Kong: from Science to Policy 76, 200–207.
862   https://doi.org/10.1016/j.atmosenv.2012.12.005

863 Li, Y., Shao, M., Lu, S., Chang, C.-C., Dasgupta, P.K., 2010. Variations and sources of
864   ambient formaldehyde for the 2008 Beijing Olympic games. Atmospheric
865   Environment 44, 2632–2639. https://doi.org/10.1016/j.atmosenv.2010.03.045

866 Ling, Z.H., Zhao, J., Fan, S.J., Wang, X.M., 2017. Sources of formaldehyde and their
867   contributions to photochemical O_3 formation at an urban site in the Pearl River
868   Delta,   southern   China.   Chemosphere   168,   1293–1301.
869   https://doi.org/10.1016/j.chemosphere.2016.11.140

870 Liu, J., Li, X., Tan, Z., Wang, W., Yang, Y., Zhu, Y., Yang, S., Song, M., Chen, S., Wang,
871   H., Lu, K., Zeng, L., Zhang, Y., 2021. Assessing the Ratios of Formaldehyde
872   and Glyoxal to NO_2 as Indicators of O_3–NO_x–VOC Sensitivity. Environ. Sci.
873   Technol. 55, 10935–10945. https://doi.org/10.1021/acs.est.0c07506

874 Lou, S., Holland, F., Rohrer, F., Lu, K., Bohn, B., Brauers, T., Chang, C.C., Fuchs, H.,
875   Häseler, R., Kita, K., Kondo, Y., Li, X., Shao, M., Zeng, L., Wahner, A., Zhang,
876   Y., Wang, W., Hofzumahaus, A., 2010. Atmospheric OH reactivities in the Pearl
877   River Delta – China in summer 2006: measurement and model results.
878   Atmospheric   Chemistry   and   Physics   10,   11243–11260.
879   https://doi.org/10.5194/acp-10-11243-2010

880 Luecken, D.J., Hutzell, W.T., Strum, M.L., Pouliot, G.A., 2012. Regional sources of
881   atmospheric formaldehyde and acetaldehyde, and implications for atmospheric
882   modeling.   Atmospheric   Environment   47,   477–490.
883   https://doi.org/10.1016/j.atmosenv.2011.10.005

884 Lui, K.H., Ho, S.S.H., Louie, P.K.K., Chan, C.S., Lee, S.C., Hu, D., Chan, P.W., Lee,
885   J.C.W., Ho, K.F., 2017. Seasonal behavior of carbonyls and source
886   characterization of formaldehyde (HCHO) in ambient air. Atmospheric
887   Environment 152, 51–60. https://doi.org/10.1016/j.atmosenv.2016.12.004

888 Monks, P. S., Archibald, A. T., Colette, A., Cooper, O., Coyle, M., Derwent, R., ... &
889   Williams, M. L. (2015). Tropospheric ozone and its precursors from the urban
890   to the global scale from air quality to short-lived climate forcer. *Atmospheric*
891   *Chemistry and Physics*, 15(15), 8889-8973.

892 Murillo, J.H., Marín, J.F.R., Román, S.R., 2012. Determination of carbonyls and their
893   sources in three sites of the metropolitan area of Costa Rica, Central America.
894   Environ Monit Assess 184, 53–61. https://doi.org/10.1007/s10661-011-1946-5

895 Pang, X., Mu, Y., 2006. Seasonal and diurnal variations of carbonyl compounds in
896   Beijing ambient air. Atmospheric Environment 40, 6313–6320.
897   https://doi.org/10.1016/j.atmosenv.2006.05.044

898 Rao, Z., Chen, Z., Liang, H., Huang, L., Huang, D., 2016. Carbonyl compounds over
899   urban Beijing: Concentrations on haze and non-haze days and effects on radical
900   chemistry. Atmospheric Environment, Air Pollution in the Beijing – Tianjin –
901   Hebei (BTH) region, China 124, 207–216.
902   https://doi.org/10.1016/j.atmosenv.2015.06.050

903 Sahu, L. K., & Saxena, P. (2015). High time-resolved volatile organic compounds
904   measurements at an urban location in India: Sources, variability, and role in
905   ozone formation. *Environmental Science and Pollution Research*, 22(5), 3975-
906   3986.

907 Schroeder, J.R., Crawford, J.H., Fried, A., Walega, J., Weinheimer, A., Wisthaler, A.,
908   Müller, M., Mikoviny, T., Chen, G., Shook, M., Blake, D.R., Tonnesen, G.S.,
909   2017. New insights into the column CH2O/NO2 ratio as an indicator of near-
910   surface ozone sensitivity. Journal of Geophysical Research: Atmospheres 122,
911   8885–8907. https://doi.org/10.1002/2017JD026781

912 Shao, M., Lu, S., Liu, Y., Xie, X., Chang, C., Huang, S., Chen, Z., 2009. Volatile organic
913   compounds measured in summer in Beijing and their role in ground-level ozone
914   formation. Journal of Geophysical Research: Atmospheres 114.
915   https://doi.org/10.1029/2008JD010863

916 Shen, X., Zhao, Y., Chen, Z., Huang, D., 2013. Heterogeneous reactions of volatile
917   organic compounds in the atmosphere. Atmospheric Environment 68, 297–314.
918   https://doi.org/10.1016/j.atmosenv.2012.11.027

919 Tan, Z., Lu, K., Jiang, M., Su, R., Dong, H., Zeng, L., Xie, S., Tan, Q., Zhang, Y., 2018.
920   Exploring ozone pollution in Chengdu, southwestern China: A case study from
921   radical chemistry to O3-VOC-NOx sensitivity. Science of The Total
922   Environment 636, 775–786. https://doi.org/10.1016/j.scitotenv.2018.04.286

923 Tonnesen, G.S., Dennis, R.L., 2000. Analysis of radical propagation efficiency to assess
924   ozone sensitivity to hydrocarbons and NO x : 2. Long-lived species as indicators
925   of ozone concentration sensitivity. Journal of Geophysical Research:

Atmospheres 105, 9227–9241. https://doi.org/10.1029/1999JD900372

Vermeuel, M.P., Novak, G.A., Alwe, H.D., Hughes, D.D., Kaleel, R., Dickens, A.F., Kenski, D., Czarnetzki, A.C., Stone, E.A., Stanier, C.O., Pierce, R.B., Millet, D.B., Bertram, T.H., 2019. Sensitivity of Ozone Production to NOx and VOC Along the Lake Michigan Coastline. Journal of Geophysical Research: Atmospheres 124, 10989–11006. https://doi.org/10.1029/2019JD030842

Wang, C., Huang, X.-F., Han, Y., Zhu, B., He, L.-Y., 2017. Sources and Potential Photochemical Roles of Formaldehyde in an Urban Atmosphere in South China. Journal of Geophysical Research: Atmospheres 122, 11,934-11,947. https://doi.org/10.1002/2017JD027266

Wang, Y., Guo, H., Zou, S., Lyu, X., Ling, Z., Cheng, H., Zeren, Y., 2018. Surface O3 photochemistry over the South China Sea: Application of a near-explicit chemical mechanism box model. Environmental Pollution 234, 155–166. https://doi.org/10.1016/j.envpol.2017.11.001

Wang, Y., Wang, H., Zhang, X., et al. (2020). Formation of secondary organic aerosols from carbonyl compounds: Insights from field observations and simulations. *Atmospheric Chemistry and Physics*, 20, 6177–6189.

Xue, L., Gu, R., Wang, T., Wang, X., Saunders, S., Blake, D., Louie, P.K.K., Luk, C.W.Y., Simpson, I., Xu, Z., Wang, Z., Gao, Y., Lee, S., Mellouki, A., Wang, W., 2016. Oxidative capacity and radical chemistry in the polluted atmosphere of Hong Kong and Pearl River Delta region: analysis of a severe photochemical smog episode. Atmospheric Chemistry and Physics 16, 9891–9903. https://doi.org/10.5194/acp-16-9891-2016

Xue, L.K., Wang, T., Gao, J., Ding, A.J., Zhou, X.H., Blake, D.R., Wang, X.F., Saunders, S.M., Fan, S.J., Zuo, H.C., Zhang, Q.Z., Wang, W.X., 2014. Ground-level ozone in four Chinese cities: precursors, regional transport and heterogeneous processes. Atmospheric Chemistry and Physics 14, 13175–13188. https://doi.org/10.5194/acp-14-13175-2014

Xue, L.K., Wang, T., Guo, H., Blake, D.R., Tang, J., Zhang, X.C., Saunders, S.M., Wang, W.X., 2013. Sources and photochemistry of volatile organic compounds in the remote atmosphere of western China: results from the Mt. Waliguan Observatory. Atmospheric Chemistry and Physics 13, 8551–8567. https://doi.org/10.5194/acp-13-8551-2013

Xue, L., Wang, T., Louie, P. K. K., Luk, C. W. Y., Blake, D. R., Gao, J., & Lee, S. H. (2013). Increasing external effects negate local efforts to control ozone air pollution: A case study of Hong Kong and implications for other Chinese cities. Environmental Science & Technology, 47(17), 10299-10305.

Yang, X., Xue, L., Wang, T., Wang, X., Gao, J., Lee, S., Blake, D.R., Chai, F., Wang, W., 2018. Observations and Explicit Modeling of Summertime Carbonyl Formation in Beijing: Identification of Key Precursor Species and Their Impact on Atmospheric Oxidation Chemistry. Journal of Geophysical Research: Atmospheres 123, 1426–1440. https://doi.org/10.1002/2017JD027403

Yang, X., Xue, L., Yao, L., Li, Q., Wen, L., Zhu, Y., Chen, T., Wang, X., Yang, L., Wang, T., Lee, S., Chen, J., Wang, W., 2017. Carbonyl compounds at Mount Tai in the North China Plain: Characteristics, sources, and effects on ozone formation. Atmospheric Research 196, 53–61. https://doi.org/10.1016/j.atmosres.2017.06.005

Ye, Z., Xie, S., Wu, Y., et al. (2021). Characterization of carbonyl compounds and their contributions to ozone and secondary organic aerosol formation in a megacity. *Environmental Science & Technology*, 55(14), 9465–9474.

Yuan, B., Chen, W., Shao, M., Wang, M., Lu, S., Wang, Bin, Liu, Y., Chang, C.-C., Wang, Boguang, 2012. Measurements of ambient hydrocarbons and carbonyls in the Pearl River Delta (PRD), China. Atmospheric Research, Remote Sensing of Clouds and Aerosols: Techniques and Applications - Atmospheric Research 116, 93–104. https://doi.org/10.1016/j.atmosres.2012.03.006

Zhang, X., Chen, Z.M., Zhao, Y., 2010. Laboratory simulation for the aqueous OH-oxidation of methyl vinyl ketone and methacrolein: significance to the in-cloud SOA production. Atmospheric Chemistry and Physics 10, 9551–9561. https://doi.org/10.5194/acp-10-9551-2010

Zhang, X., Wu, Z., He, Z., Zhong, X., Bi, F., Li, Y., Gao, R., Li, H., Wang, W., 2022. Spatiotemporal patterns and ozone sensitivity of gaseous carbonyls at eleven urban sites in southeastern China. Science of The Total Environment 824, 153719. https://doi.org/10.1016/j.scitotenv.2022.153719

Zhang, Y., Wang, X., Wen, S., Herrmann, H., Yang, W., Huang, X., Zhang, Z., Huang, Z., He, Q., George, C., 2016. On-road vehicle emissions of glyoxal and methylglyoxal from tunnel tests in urban Guangzhou, China. Atmospheric Environment 127, 55–60. https://doi.org/10.1016/j.atmosenv.2015.12.017

Zhang, Z., Zhang, Y., Wang, X., Lü, S., Huang, Z., Huang, X., Yang, W., Wang, Y., Zhang, Q., 2016. Spatiotemporal patterns and source implications of aromatic hydrocarbons at six rural sites across China's developed coastal regions. Journal of Geophysical Research: Atmospheres 121, 6669–6687. https://doi.org/10.1002/2016JD025115

Zhou, Z., Tan, Q., Deng, Y., Lu, C., Song, D., Zhou, X., Zhang, X., Jiang, X., 2021. Source profiles and reactivity of volatile organic compounds from anthropogenic sources of a megacity in southwest China. Science of The Total Environment 790, 148149. https://doi.org/10.1016/j.scitotenv.2021.148149